

Time domain analysis procedures for fatigue assessment of a semi-submersible wind turbine

Marit I. Kvittem^{*1,2} and Torgeir Moan²

¹*NOWITECH, Norwegian University of Science and Technology, Trondheim, Norway*

²*CeSOS, Norwegian University of Science and Technology, Trondheim, Norway*

September 18, 2014

Abstract

Long term time domain analysis of the nominal stress for fatigue assessment of the tower and platform members of a three-column semi-submersible was performed by fully coupled time domain analyses in Simo-Riflex-AeroDyn. By combining the nominal stress ranges with stress concentration factors, hot spot stresses for fatigue damage calculation can be obtained. The aim of the study was to investigate the necessary simulation duration, number of random realisations and bin sizes for the discretisation of the joint wind and wave distribution. A total of 2316 3-hour time domain simulations, were performed.

In mild sea states with wind speeds between 7 and 9 m/s, the tower and pontoon experienced high fatigue damage due to resonance in the first bending frequency of the tower from the tower wake blade passing frequency (3P).

Important fatigue effects seemed to be captured by 1 hour simulations, and the sensitivity to number of random realisations was low when running simulations of more than one hour. Fatigue damage for the tower base converged faster with simulation duration and number of random realisations than it did for the platform members.

Bin sizes of 2 m/s for wind, 1 s for wave periods and 1 m for wave heights seemed to give acceptable estimates of total fatigue damage. It is, however, important that wind speeds that give coinciding 3P and tower resonance are included and that wave periods that give the largest pitch motion are included in the analysis.

Keywords: offshore wind, semi-submersible, integrated analysis, fatigue

1 Introduction

Fatigue damage is known to be a problem for bottom fixed offshore wind turbine substructures, and is also expected to be significant to floating wind turbines (FWTs). Adequate fatigue strength should be ensured by design. Wind parks consist of units with similar designs, and are thus vulnerable to “common cause”

*marit.irene.kvittem@ntnu.no

failures, which means that the economic consequences of poor fatigue design are serious. It is important, therefore, to make good fatigue estimates early in the design process.

Whereas for a wave only case, environmental conditions are taken from a scatter *table* (two variables: wave height and period), environmental conditions for a combined wind and wave case have to be taken from a scatter *block* (three variables: wind speed, wave height and period). This increases the number of combinations of wind and sea states that needs to be included in the fatigue damage assessment significantly compared to an onshore turbine or a traditional offshore structure. Wind- and wave directions and current are additional parameters that further increase the number of load cases.

The equations of motion for a wind turbine on a compliant sub-structure has many non-linear contributions: Catenary mooring line forces, viscous and aerodynamic forces and large displacements that require the loads to be calculated at the updated position. Due to these non-linearities the wind and wave loads on the structure cannot be treated separately, which means that all combinations of wind and wave loads must be analysed individually. Analysis of a non-linear system must also be performed in the time-domain, which is much more computationally time consuming than in the frequency domain.

Another issue is the discrepancy between guidelines for onshore wind turbines and for floating platforms when it comes to simulation length requirements. Due to the long natural periods of a compliant floating platform, it is often necessary to simulate from 3 to 6 hours to capture slowly varying response to wave and wind loads. This is emphasized in the new offshore standard for floating wind turbines from DNV [1]. Fixed wind turbines have higher natural frequencies, and the slowly varying response will be static, thus the normal simulation time for wind turbines is ten minutes. It is also common practice to assume ten minute stationary wind in wind statistics, whereas it is 1 to 6 hours for waves. Karimirad and Moan [2] found that a minimum of 3 hour simulations were needed to capture extreme bending moments for a 5 MW spar turbine, unless proper extrapolation was used. However, extreme values relate to the ultimate limit state, and do not normally contribute to fatigue due to the high return period.

In summary, all of these factors lead to a large number of environmental conditions that need to be simulated in the time domain for one to 6 hours. Also, to account for statistical uncertainty, a number of different realisations of the wind and wave histories must be included in the fatigue assessment. This requires unrealistic amounts of computing capacity and time in the design phase, and is the motivation for studying the parameters that make the execution time so long.

A recent paper by Haid et al. [3] studied the effect of simulation length on fatigue and ultimate loads for the OC3 spar buoy wind turbine, and concluded that the fatigue damage in the tower, blades and mooring system was more sensitive to the treatment of residuals in rainflow cycle counting than to simulation length. This work was done using the non-linear aero-hydro-servo-elastic tool FAST.

Earlier work by the authors [4], analyses applying the simplified aerodynamics model TDHmill in combination with Simo-Riflex indicated that 6-7 realisations of 1-hour wind and wave histories will give a fatigue estimate close to the damage based on the average of 10 3-hour realisations. This was, however,

based on a limited number of environmental conditions.

The current study aims at assessing simulation requirements for fatigue damage estimation, and the key questions are:

- How many realisations are needed to capture the effect of statistical uncertainty?
- What simulation duration is necessary to capture the important effects of slowly varying loads?
- What is the maximum bin size for the discretisation of the joint wind and wave distribution?

Fatigue for a a three column, catenary moored semi-submersible with the NREL 5MW [5] supported by the OC3 tower [6] (see Fig. 1) was examined. The single semi-submersible wind turbine (SSWT) was inspired by WindFloat [7]. The simulation tool used was Simo-Riflex-AeroDyn from Marintek and CeSOS. 10 realisations of 197 3-hour environmental conditions were simulated, with a CPU time approximately twice real time. The environmental conditions were strategically chosen from a joint wind and wave distribution to identify special expected and unexpected load effects.

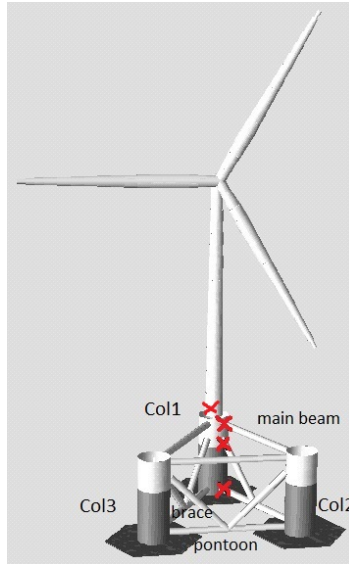
These simulations serve as basis for comparisons of the fatigue damage for varying simulation lengths (from 10 minutes to 3 hours) and for varying number of realisations (1 to 10) of the same environmental conditions. The results were also used to identify load cases and effects that contribute significantly to fatigue, and to examine the effect of increasing the bin sizes for load case selection. The effect of misaligned wind and waves was also examined.

2 Modelling of the semi-submersible wind turbine and loads

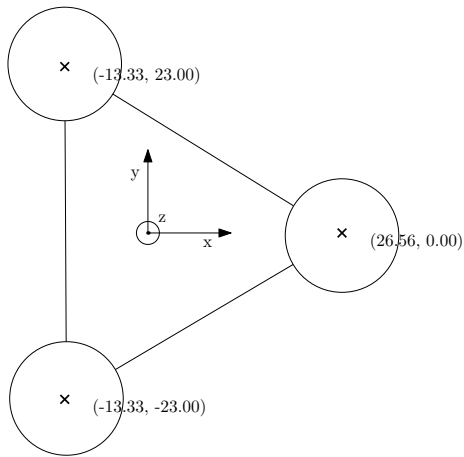
2.1 Platform description

The WindFloat concept was chosen as inspiration for the floating platform in this study, and the platform geometry given in [7] was kept, but since more detailed specifications than what is available was necessary, a different design with similar global characteristics was developed (Tab. 2). The new platform was developed to have a mass distribution similar to WindFloat, but no extensive design check was performed on the assumed wall thicknesses. Compared to the OC4 DeepCWind concept, which is also a semi-submersible wind turbine concept, the column plate thicknesses for this design are smaller, while the braces and pontoons have thicker plates. The brace dimensions for the DeepCWind platform were found sufficient in an initial design check [17] for the central North Sea. Specifications for the turbine, the NREL 5MW reference turbine, can be found in [5], and in [6] for the tower.

The control system constants from the OC3 Hywind spar study were applied [6], with a constant torque strategy above rated wind speed. This controller is tuned to avoid negative damping above rated wind speed due to the pitch motion of the OC3 Hywind platform. This was done by setting the control system natural frequency to 0.2 rad/s, which is outside of the wave frequency



(a) Structural model. Locations for which fatigue results are presented in Sec. 6 are marked with 'x'.



(b) Top view. The coordinate system $z = 0$ is in the mean water line.

Figure 1: Semi-submersible wind turbine.

range and below the natural pitch frequency of the spar platform. 0.2 rad/s is above the natural pitch frequency of the SSWT (0.17 rad/s) in this study, but setting control constants to get below this will give too much variation in the power production. Even though the controller natural pitch frequency could not be set below this limit, applying the OC3 Hywind constants gave less pitch motion than the land based controller. The negative damping instability was not observed for this platform, probably due to the heave plates, which provide viscous damping for pitch motion.

Table 1: Mass, damping and restoring data. All values are given for the platform without the turbine (rotor-nacelle-assembly and tower), unless otherwise noted, and are valid for zero thrust force ballast condition.

Displacement with WT	4810e6 <i>kg</i>
Mass with WT	4619e6 <i>kg</i>
Centre of gravity with WT	(-0.331 <i>m</i> , 0.0 <i>m</i> , 1.489 <i>m</i>)
Mass	4019e6 <i>kg</i>
Centre of gravity	(-4.300 <i>m</i> , 0.0 <i>m</i> , -7.857 <i>m</i>)
Radius of gyration Rxx	22.29 <i>m</i>
Radius of gyration Ryy	19.62 <i>m</i>
Radius of gyration Rzz	26.06 <i>m</i>
Radius of gyration Ryz	4.69 <i>m</i>
Hydrostatic stiffness Heave	2445 <i>kN</i>
Hydrostatic stiffness Roll	749815 <i>kNm</i>
Hydrostatic stiffness Pitch	7548571 <i>kNm</i>

2.1.1 Mooring

The platform is positioned by four mooring lines, two lines attached to column 1 and one line attached to each of the two other columns. In order to get natural periods for surge, sway and yaw close to what is specified for the generic WindFloat, a new mooring system was designed. A simple Reflex mooring line model was used, together with the mooring line equations in Ref. [18], to achieve the desired stiffness. The lines have 60 m of chain on top, 30 tonnes, 3.8 m³ clump weight between chain and polyester rope, 769.8 m of polyester rope in the middle and 232.58 m of chain at the bottom.

2.1.2 Ballast system

The WindFloat platform has an active ballast system to keep the turbine upright and thus maximise power output as the wind direction and intensity change. This is done by pumping water ballast between the columns with a reaction time of 20 minutes [7] to significant changes in the mean wind speed and direction. The function of the ballast system is illustrated in Fig. 2 .

The initial ballast in the SSWT in these analyses was distributed to account for the asymmetric loading of the platform, i.e. the weight of the turbine and mooring system. During operation, the mean thrust force, tower drag and rotor torque give the platform a constant tilt. To get an upright configuration of the

Table 2: Fairlead and anchor line positions.

	x	y	z
Fairlead 1	31.56	0	-17
Fairlead 2	-15.78	-27.33	-17
Fairlead 3	-15.78	27.33	-17
Fairlead 4	31.56	0	-17
Anch 1	738.07	-706.51	-320
Anch 2	-721.76	-733.31	-320
Anch 3	-721.76	733.31	-320
Anch 4	738.07	706.51	-320

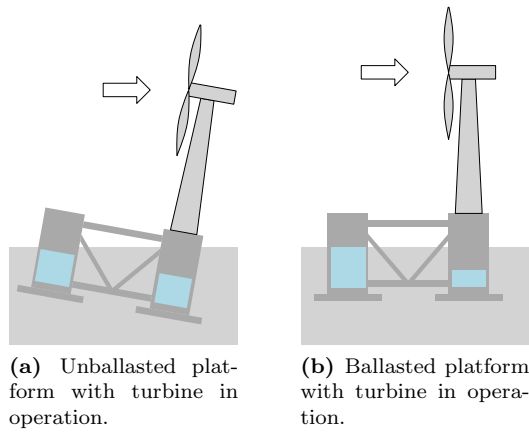


Figure 2: Illustration of ballast system.

platform in operation, a ballast system was modelled. Since the reaction time of the ballast system is long compared to other the dynamic loads on the system, it was modelled as constant ballast, and a new ballast distribution was calculated for every mean wind speed. Thus, mass distribution and restoring was updated for each environmental condition. The ballast distribution between column 1 and columns 2 and 3 (see numbering in Fig. 1a) was calculated from the thrust force and tower drag for constant wind velocity with a power law wind shear. The ballast distribution between column 2 and column 3 was calculated based on the rotor torque.

Table 3: Mass distribution for different wind speeds. Mass and vertical position of the centre of gravity (z_G) are given for the column, including heave plates and ballast.

U_{hub} (m/s)	Column 1 Mass (kg)	z_G (m)	Column 2 Mass (kg)	z_G (m)	Column 3 Mass (kg)	z_G (m)
0.0	749,418	-10.358	1400,128	-7.918	1400,128	-7.918
8.0	658,582	-10.439	1441,151	-7.715	1449,940	-7.671
11.2	579,217	-10.384	1476,078	-7.539	1494,378	-7.446
25.0	659,277	-10.439	1435,887	-7.741	1454,509	-7.648
49.0	652,823	-10.440	1448,425	-7.678	1448,425	-7.678

Samples of masses and centre of gravity for different wind speeds are presented in Tab. 4. In the cases with wind coming in from the side, where the rotor was rotated to be perpendicular to the wind, the same methodology to balance the thrust force and torque was used.

2.1.3 Eigenperiods

Some important eigenperiods (damped), found by decay analyses of the no thrust force ballast condition, are listed in Tab. 5. The tower first fore-aft bending frequency is higher than the fixed NREL 5 MW tower frequencies, and in this case that means that it will be within the range of the blade passing frequencies for lower wind speeds. This would normally call for a redesign of the tower. However, the analyses performed for this paper were also used in a comparison study of fatigue for different FWT concepts, where the same turbine and tower were used on different floating platforms [19]. In Ref. [19], the resonance effect was seen also for a TLP and the semi-submersible used in the OC4 study [20]. Thus, instead of optimising the design, it seems relevant to keep this standard design and highlight the issue.

2.2 Coupled analysis code

The coupled analysis tool Simo-Riflex-AeroDyn was applied in this study. Simo-Riflex from Marintek ([8], [9]) is suitable for time domain simulations of floating rigid bodies (Simo) coupled to flexible beam elements (Riflex).

The structural model of the turbine tower, blades and shaft was made up by beam elements. The rotor speed and the power output were controlled by a generator torque controller a blade pitch controller, respectively. Aerodynamic forces on the blades were calculated by AeroDyn [10], which reads a turbulent

Table 4: Damped natural periods for the platform ballasted for a zero wind condition.

Mode	T (s)
Surge	107.0
Sway	124.8
Heave	19.9
Roll	35.6
Pitch	37.4
Yaw	68.5
Tower 1st	2.3

wind field and applies the aerodynamic nodal loads to the blade elements. This method was verified by Ormberg and Bachynski [11].

Simo [12] solves the equation of motion in time domain for a single or multiple rigid bodies based on a frequency domain solution of the hydrodynamic loads by a panel method code (e.g. Wadam [13]). In addition, viscous forces can be included by a drag formulation. The traditional modelling method is to assume the complete platform as a rigid body. However, internal member forces of a statistically indeterminate structure can not be extracted from such an analysis. Thus, in order to get forces in the braces, the three columns of the platform were modelled as individual Simo bodies with potential theory forces, and the connecting braces were modelled as Riflex beam elements with Morison type forces.

2.3 Hydrodynamic forces

2.3.1 Potential theory model for columns and heave plates

The dynamic equilibrium equation for the columns (and heave plates) include mass forces, hydrostatic stiffness, gravity, buoyancy, external forces from Riflex, retardation functions accounting for frequency dependent added mass and linear damping, and wave excitation forces.

Wave force transfer functions according to the potential theory and the retardation functions for the columns with heave plates were obtained using multi body analysis in Wadam [13]. The heave plates were modelled by assuming a flat plate at the bottom of the columns in the Wadam analysis.

Hydrodynamic interaction between the columns was taken into account by applying the multi body analysis. However, some limitations on hydrodynamic interaction are inherent in the coupled Simo-Riflex software. This means that for one body, the effect of the presence of the other bodies was included in the force transfer functions and retardation functions, but the effect of motion of the other bodies was only accounted for in the force transfer functions, not in the retardation functions. The wave forces from Wadam include Froude-Krylov (\mathbf{F}^{FK}) and diffraction (\mathbf{F}^D) forces, as shown in Eq. 1.

$$\mathbf{F}^{HYD} = \mathbf{F}^{FK} + \mathbf{F}^D \quad (1)$$

In addition to the wave forces according to linear potential theory, viscous drag forces were included for both the columns and the heave plates. The drag

terms were calculated as described in the following section. The total wave forces in 6 degrees of freedom then becomes a sum of Froude-Krylov, diffraction and drag forces.

Difference frequency force transfer functions were not included since these are computationally very expensive to find in a multibody panel model analysis. A single body analysis in Wadam showed that the difference frequency forces for this platform are most predominant in surge and sway. These motions can contribute to fatigue, but in the current study excluding second order wave forcing was a trade-off for being able to calculate fatigue damage in the platform members.

2.3.2 Morison force model for beams, pontoons and braces

The wave forces on the slender beams, braces and mooring lines were calculated by Morison's formula (Eq. 2). The equation shows how the axial, lateral or transversal force, dF acting on a strip of the member, in its local coordinate system, are expressed in the simulations.

$$dF = \rho A \dot{u} + \rho A C_m (\dot{u} - \ddot{r}) + \frac{\rho}{2} D C_d |u - \dot{r}| (u - \dot{r}) \quad (2)$$

A is the cross section area, D is the reference area normal to the flow direction, i.e. the outer diameter for a circular cross section and the heave plate area for heave motion of the heave plates, and ρ is the seawater density. u is the wave particle velocity and r is the local member displacement, both in the direction of the force. C_d is the non-dimensional drag term, which is direction specific and C_m is the added mass coefficient, which is assumed to be zero for the longitudinal direction.

Table 1 shows the C_m and C_d coefficients applied in the analysis. For the mooring chains the non dimensional drag coefficients were taken from DNV-OS-E301 [14]. A drag coefficient of 1.0 for the columns was chosen to get a conservative estimate of the excitation forces on the columns. This value is higher than recommended in DNV-RP-C205 [15] for fixed cylinders, and may not give conservative damping values in surge and sway motions. Therefore, a sensitivity analysis comparing fatigue damage in the tower and braces was carried out with a drag coefficient of 0.7 for the columns, at relevant wave periods. This analysis gave less than 1.5% difference in all cases, and provided confidence that the results are not sensitive to the column drag coefficient. In heave, pitch and roll, the heave plates contribute to most of the hydrodynamic damping for this platform.

Vertical Morison drag terms for the heave plates and transversal/lateral drag terms for the columns were calculated by the last term in Eq. 2. The heave plate drag coefficient in Tab. 1 is based on model tests and numerical analysis of the WindFloat concept [16].

2.4 Aerodynamic loads in low wind speeds

At low wind speeds, wake dynamics can be significant. AeroDyn has the option of calculating the aerodynamic loads by simple BEM or by a generalized dynamic wake (GDW) model. The BEM method in AeroDyn does not include a dynamic wake correction, although it exists in other codes using BEM. In addition to

Table 5: Non-dimensional quadratic drag and added mass coefficients. For columns and heave plates added masses are found by potential theory.

Component	Transverse C_d (-)	Longitudinal C_d (-)	C_m (-)
Columns	1.0	0.0	-
Mooring chain	2.4	1.15	1.0
Mooring polyester rope	1.6	0.0	1.0
Main beam and pontoons	1.0	0.0	1.0
Braces	1.0	0.0	1.0
Heave plates	7.5	0.0	-

accounting for wake damping, GDW has the advantage of less computation time than BEM. The validity of the GDW model, however, is limited to higher wind speeds (unstable behaviour is reported for axial induction factors above $1/3$, observed at 8 m/s and below for certain fixed turbines [10]). A floating wind turbine will pitch and surge, which affects the relative wind speed, and hence it will move in and out of the unstable range of GDW at wind speeds close to the limit (8 m/s).

This lead to unphysical instabilities in the analyses with particular combinations of waves and wind timeseries at 9 m/s. By changing to BEM, this effect was avoided.

However, between 7 and 9 m/s tower resonance due to the blade passing frequency (3P) load was observed, which led to high fatigue damage for these cases. Damping determines the amplitude of resonant behaviour, and damping may be lost or gained by including the dynamics of a wake. In a comparison between a simulation with BEM and one with GDW, without the unstable behaviour, GDW gave significantly less fatigue for 9 m/s wind. Since this damping is very important for the outcome of this study, and since the authors believe that GDW gives a more physical representation of the aerodynamic loads at this wind speed, GDW was used for the 9 m/s case. The few unstable analyses were rerun with a different wind seed. For the 7 and 8 m/s case the rotor would be too highly loaded, which would result in too many unstable analyses. Instead, tower structural Rayleigh damping was increased from a stiffness proportional coefficient 0.001 to 0.002, values which correspond to damping ratio of 0.3% and 0.6%, respectively, at the tower first fore-aft bending frequency. The original OC3 tower specifies a structural damping ratio of 1.0%, which is constant for all frequencies. Since only Rayleigh damping was available in the structural solver used in this study, damping ratio was initially chosen to be 1.0% between the first and second bending mode of the tower. Doubling the stiffness proportional stiffness gives a damping ratio close to and below what was specified for the OC3 tower, and is thus considered a conservative value.

3 Environmental data

3.1 Joint wind and wave distribution

In a study under the combined wind and wave power unit project, Marina Platform, joint wind and wave distributions for five sites in European waters were established [21], based on hindcast data of 1-hour averaged sea states and wind. The WindFloat prototype is located in the Atlantic Sea, off the coast of Portugal. Thus, the chosen environmental probability distribution of 1-hour sea states applied in this analysis was taken from the Buoy Cabo Silleiro site, off the coast of northern Portugal.

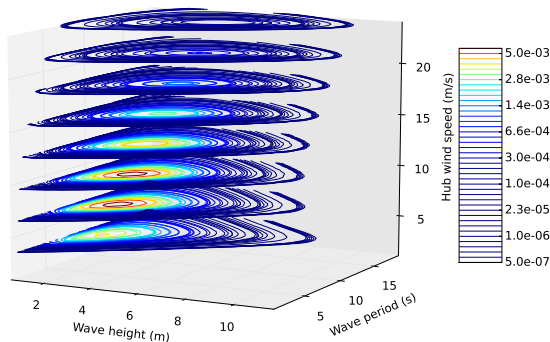


Figure 3: Joint wind and wave distribution.

3.2 Simulation length, wind and wave loads

Each environmental condition was simulated in Simo-Riflex-AeroDyn for 3 hours, plus 350 seconds warm up and transient, with 10 different stochastic samples of wind and wave timeseries. The 350 seconds of warm up and transient response contains 50 seconds controller warm up and 150 seconds of constant wind, and were removed from the results before post processing.

64-bit TurbSim [22] was used to simulate the 3-hour turbulent wind field. Turbulence was generated applying the Kaimal spectrum and the IEC normal turbulence model [23] with a reference turbulence intensity of 0.12. A power law wind shear profile with exponent of 0.14 was used for the mean wind speed component.

Since the power spectrum for wind measured over longer periods has small variations in the 1-hour range [24], it seems to be valid to assume 1 hour stationary wind fields. More recent research suggests that this gap does not exist [25], but the assumption has proven to give satisfactory models in the wind industry [26]. For fatigue analysis the very low-frequency variation from 1-3 hour changes in the wind, will most likely not have any impact compared to the high-frequency variations.

Irregular waves were generated in Simo with a 3-parameter Jonswap spectrum with a peak factor of 3.3, using Airy linear wave theory [12]. Long crested

waves were assumed. The misaligned wind and wave cases are described in Sec. 5.

4 Fatigue damage calculation

Axial stress σ in net cross sections of the different structural members was calculated for 24 points around the circumference of the pipe cross sections. The base metal cross sections of the members were used in the stress calculation and it was assumed that hot spot stress amplitudes are proportional to the nominal member stresses. Since it was the effects of simulation parameters that were under investigation in this study, an SCF of 1.0 was applied (the actual hot spot stress is proportional to this value). For a more detailed study with for multi axial stress conditions, possible different SCFs for different stress components need to be considered.

Nominal axial stress was calculated according to Eq. 4 [27]. Figure 4 shows the definitions of directions and axis for the tower base.

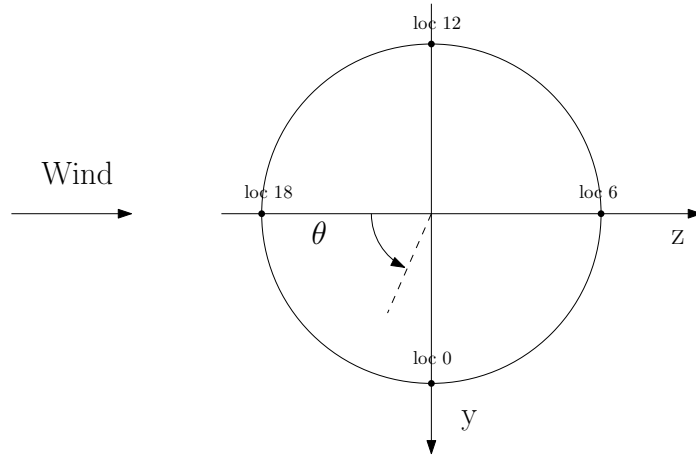


Figure 4: Top view of tower base cross section.

$$\sigma = \frac{N_x}{A} + \frac{M_y}{I_y} r_1 \cos \theta - \frac{M_z}{I_z} r_1 \sin \theta \quad (3)$$

N_x is the axial force, A is the nominal cross sectional area, M_y and M_z are bending moments and I_y and I_z are the sectional moments of area.

Rainflow counting was performed for the stress timeseries and fatigue was calculated by S-N-curves from DNV [28] and Miner's sum. Residual half cycles from the Rainflow counting were counted as half amplitudes.

Since fatigue damage occurs in welds rather than in the base material, S-N curves for girth welds were used. Based on the joint geometry, S-N curve D for σ was chosen, with categories "air" for tower and "cathodic protection" for the other members. The offshore wind turbine standard DNV-OS-J101 [29] states that the "in seawater with cathodic protection" curve can be used for members in the splash zone and water, assuming no repair and a guaranteed coating life of 15 years. In this study the service life is 20 years, but since the aim of the

study was not to perform fatigue design, the 15 year coating lifetime rule is disregarded.

To find the total damage over a service life of 20 years, damage estimates were multiplied by the respective probability and a scaling factor to adjust for the fact that the probability distribution yields for 1-hour sea states (T^{distr}) (see Eq. 4).

In traditional summations of fatigue damage, the probability is multiplied by the bin volume to achieve a total probability of 1. When the environmental conditions are not equally spaced, which was the fact in this study, it is not possible to find a bin volume, thus the scaling factor $p^{tot} / \sum_{i=1}^{N^{lc}} p_i$ was introduced instead. For the study of simulation length requirements and the number of stochastic samples, this factor cancels out, since damage for the same environmental conditions are compared, thus the factor will be a constant.

$$D_{total} = N^{20yr} \frac{p^{tot}}{\sum_{i=1}^{N^{lc}} p_i} \frac{T^{distr}}{T^{sim}} \frac{1}{N^{seeds}} \sum_{i=1}^{N^{lc}} \sum_{j=1}^{N^{seeds}} D_{ij} p_i \quad (4)$$

In Eq. 4, D_{total} is the accumulated damage over 20 years for the included environmental conditions, p^{tot} is the total probability of all load cases within the operation range of the turbine and with a probability above 10^{-4} , p_i is the point probability of environmental condition i , N^{20yr} is the number of 1-hour sea states in 20 years, N^{seeds} is the number of realisations of wind and waves, N^{lc} is the number of environmental conditions in the analysis, D_{ij} is the damage for a simulation for realisation number j of environmental condition i , with duration T^{sim} . T^{distr} is the averaging period for the applied joint wind and wave distribution, i.e. 1 hour.

Since this study focused on a turbine in operation, it was assumed that it will be in operation the whole time during wind conditions between cut-in and cut-out wind speeds. This is, of course, not a realistic assumption, but an operation time factor will not affect the results in this study. For a full lifetime fatigue assessment, downtime, along with survival, fault and installation, must also be included in separate analyses.

5 Load case selection

The IEC standard for design requirements for offshore wind turbines [30] recommends the following bin size for joint wind and wave assessment:

- Mean wind speed: 2 m/s
- Significant wave height: 0.5 m
- Peak wave period: 0.5 s

The DNV standard for column stabilised units [31] specifies that fatigue limit state analysis should cover events down to a probability level of 10^{-4} .

If the recommended bin sizes are used the total number of environmental conditions that have a marginal probability higher than 10^{-4} is 1539, not accounting for the directionality of wind or waves. Each load case must be simulated for at least 3-hours and with a certain number of different seeds for

random phase angles to capture worst representative wave loads. This requires excessive simulation time and capacity.

The number of random seeds required by the IEC standard [30] is 6. But since the structural response of a FWT to environmental loads is very different from a fixed structure, more variability in the response statistics is a possible outcome of these analysis. Thus, with the intention of being able to see convergence in the results, the number of seeds was increased to 10.

In this study, simulations were carried out in three phases: The first covered the necessary simulation length and number of seeds, the second covered wind-wave misalignment. After analysing the results from the first phase, additional environmental conditions were added for the study of environmental condition bin size in the third phase. A total of 2316 simulations were carried out:

- 3-hour realisations of 155 different environmental conditions with aligned wind and waves (10 seeds)
- 3-hour realisations of 42 environmental conditions with misaligned wind and waves (10 seeds)
- Additional 3-hour realisation of 346 different environmental conditions (1 seed, only used for studying the effect of bin size)

5.1 Phase 1 - Environmental conditions for simulation lengths and number of seeds

The present analysis was based on the recommended bin sizes for waves from the IEC standard, and the lower an upper turbine operation wind speed limits, together with 1 m/s bins for mean wind speed. Applying the 10^{-4} probability threshold together with turbine operation range limits, leaves 2201 load cases that have a total accumulated probability of 81%. From these, 155 environmental conditions (see Fig. 5) were selected to reflect different load case groups:

1. Base case with large bin sizes
2. 5% most probable load cases
3. Special cases with critical frequencies
4. Variation in wave height
5. Variation in wave period
6. Variation in wind/wave misalignment

As a first step, a few load cases are selected as base cases, shown as “Base case” in Fig. 5. The basic assumption in selecting these cases is that fatigue damage increases with wave height (given wave period) and that important dynamic effects are captured. A coarse grid of mean wind speeds and wave periods was selected from the 2201 load cases with probability above 10^{-4} .

The 11 most probable environmental conditions were also chosen. The reason for not including more is that one obtains many cases with low wind speed and small waves and not much variation between the cases.

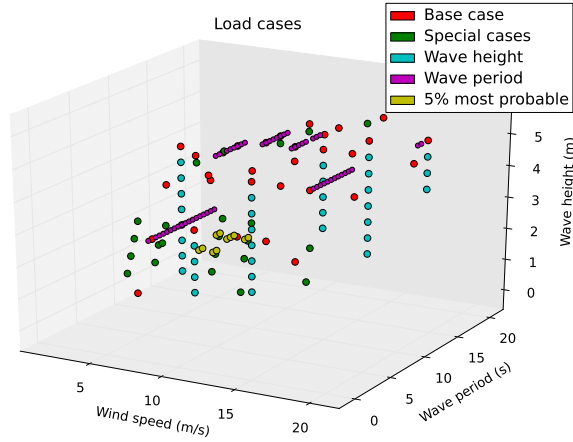


Figure 5: The 155 environmental conditions analysed in this study. Wind speed refers to hub wind.

To find how fatigue damage varies with wave height, some of the base cases were run with varying wave height. The load cases were chosen such that different wind speeds and peak periods were represented in the selection.

There are certain dynamic effects, which depend on wave period and wind speed, that can cause large fatigue damage. To make sure that these were included in the analyses, loads that might increase fatigue loading were identified:

- Wave length corresponding to when wave forces have 180 degree phase difference on columns, in this case 7.2 s and 7.7 s
- Heave resonance at 19.9 s
- Tower wake 3P loads close to tower first mode fore-aft and side-to-side bending at 2.3 s, which corresponds to mean wind speeds around 7 m/s
- Higher harmonics of drag forces (mainly 3ω) close to structural flexible modes. Most relevant wave periods give 3ω in a range between rigid body modes and the tower first bending mode, and other flexible natural frequencies are expected to be higher, so only the shortest periods are relevant to capture this phenomenon.
- Higher turbulence intensity at lower wind speeds
- Rated wind speed for maximum thrust force on rotor

Based on these criteria, combinations of wave peak periods 2.5, 6.5, 7.0, 7.5, 8., 16., 20 s and mean wind speeds 3., 5., 9., 11., 15., 23 m/s were chosen from the 1539 load cases mentioned above. From these, combinations with the largest wave height were chosen as the first step to screen load cases.

5.2 Phase 2 - Environmental conditions for wind-wave misalignment

When wind and waves come from different directions, tower bending moments can increase from the aligned case since the rotor no longer provides damping

for wave excitation. This has been documented through analyses for offshore turbines with monopile foundations [32], and is also expected to be a problem for floating wind turbines [33]. In the current study, some of the base cases were run with misaligned wind and waves ($0\text{-}90^\circ$), both with head wind and wind from the side with the rotor yawed 90° (see Fig. 6). Since a joint wind and wave distribution with directional distribution did not exist for this site, and since including directions will drastically increase the number of load cases, the misaligned wind and wave cases were only performed to check the validity of assuming unidirectional wind and long crested waves.

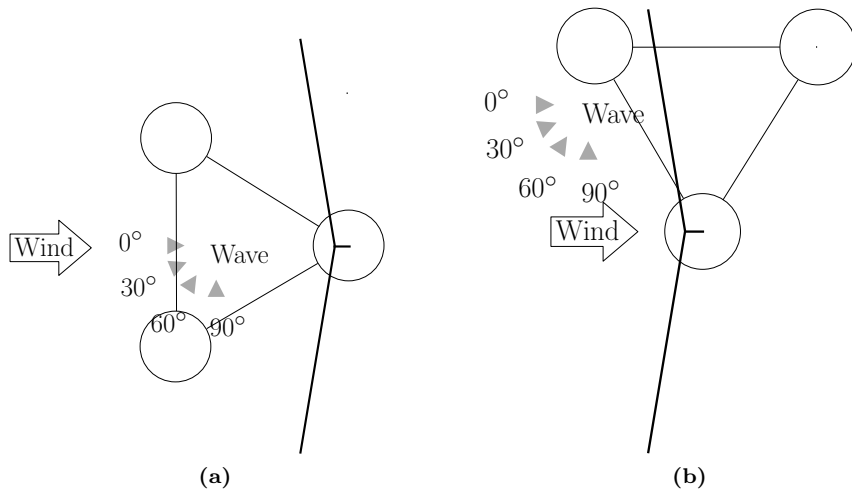


Figure 6: Top view illustration of wind and wave directions for the misaligned cases.

The turbine has a yaw mechanism to make the rotor plane normal to the wind, and since the mass and restoring properties of the platform are not symmetric, wind coming from a different direction than the one assumed in this study, causes different load responses. To get an impression of the effect of wind direction, the misalignment cases were also run for wind from the side (incoming wind angle of 90°). When wind comes from the side, it will cause the platform to yaw. Reflex can not yet model the yaw mechanism, but the rotor should be kept normal to the wind, thus the platform was given an initial yawed position, calculated based on the thrust force for a fixed turbine. This was not done for yaw due to waves, since this yaw moment was observed to be significantly lower than the yaw due to an eccentric thrust force.

5.3 Phase 3 - Environmental conditions for bin size evaluation

Since the results from the load cases listed above showed that determining fatigue damage from only 1 realisation of a 3-hour environmental condition gave reasonable estimates, one 3-hour realisation of evenly spread load cases were performed to be able to say something about the discretisation of the environmental conditions when calculating the total fatigue damage.

346 additional load cases were run, using a bin size of 1 m/s for wind speed, 1.5 m for wave height and 1 s for wave period. These load cases were only used

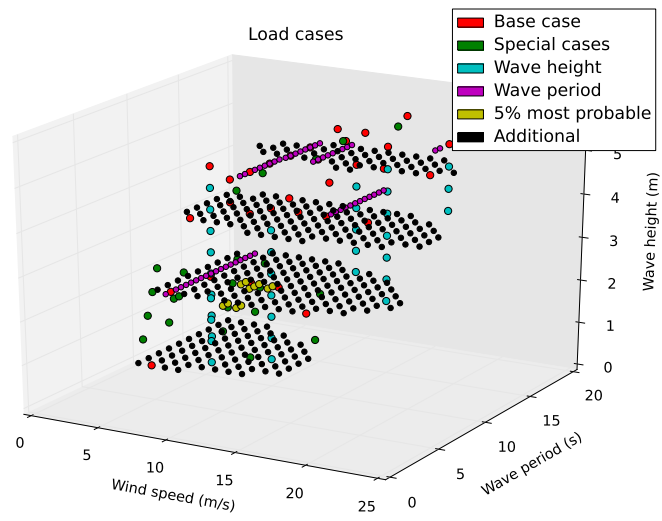


Figure 7: 346 additional environmental conditions, used for studying the effect of bin size. Only one 3-hour realisation of the additional environmental conditions was run.

to study how load case selection and bin sizes affect the total fatigue damage estimate. The additional load cases, together with the original load cases, are shown in Fig. 7.

6 Simulation results

Fatigue damage was calculated for both axial and shear stress components, but shear stress fatigue damage was significantly lower than for axial stress. Thus, the shear stress fatigue was excluded from the paper.

All results presented in this section refer to the cross section location with the maximum 10-seed average damage. The points where fatigue was calculated for the different members are shown in Fig. 1.

6.1 Load conditions that cause large fatigue damage

Wind speeds 7 m/s and 9 m/s caused high short term fatigue damage (Fig. 8) compared to what one would expect for mild wind conditions. For the higher wind speed cases (17 m/s and 20 m/s) fatigue damage is also high, but for these cases wave height is higher, thus higher damage was expected.

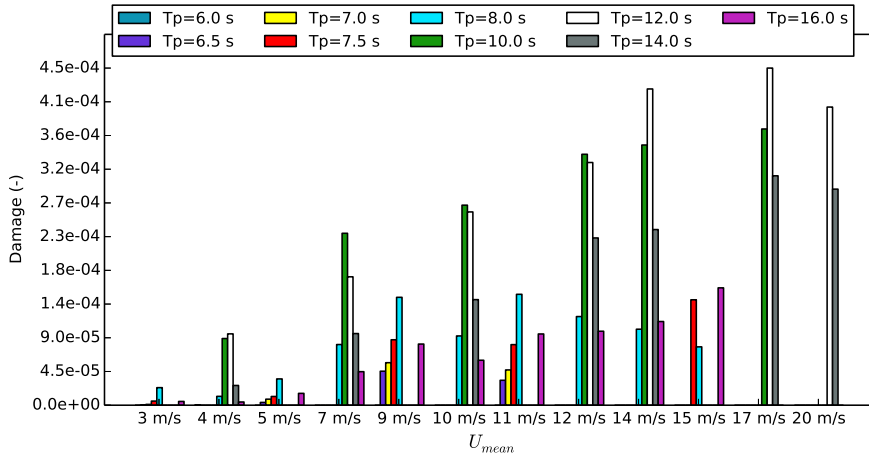


Figure 8: 3-hour fatigue damage in tower bottom for base case and special cases, arranged by wind speed and wave period. Wave heights vary between 0.5-4.5 m for below rated wind and 2.5-5.5 m for above rated wind.

Tower wake 3P loads at low wind speeds (approximately 2.67 rad/s for 7 m/s and 3.26 rad/s for 9 m/s) are close to the tower first bending mode (2.73 rad/s). This results in resonance in the tower at low wind speeds, which causes high fatigue damage. The contribution from these load cases is large in the long term fatigue analysis since this range of wind speeds occurs frequently.

This is normally not a problem for fixed foundations since the tower natural frequency is lower. The natural frequency is lower both because there are no rigid body modes and because towers are normally longer than for floating platforms. For a floating platform, there is a risk that the first bending frequency of the tower is within the three times rotational speed of the rotor in the below rated operating state.

6.2 Simulation length and number of random realisations

The total 20 year fatigue damage was calculated by Eq. 4 for the environmental conditions in Fig. 5. The number of samples varied from 1 to 10 and simulation lengths were varied from 10 minutes to 3 hours. The 10 min to 2 hour simulations were obtained by sampling stress histories from the steady state 3-hour timeseries. The fatigue damages calculated based on 10 min to 2 hour durations were scaled up for comparison with 3 hour damages.

Estimating the total 20 year fatigue based on 10x1-hour simulations of each load case underestimated damage by less than 5% compared to 10x3-hour simulations (Fig. 9). Using 10x10-minute simulations underestimated the damage by 12%. Fatigue damage for the tower appeared to be less affected by simulation length than the platform members, pontoon, main beam and brace.

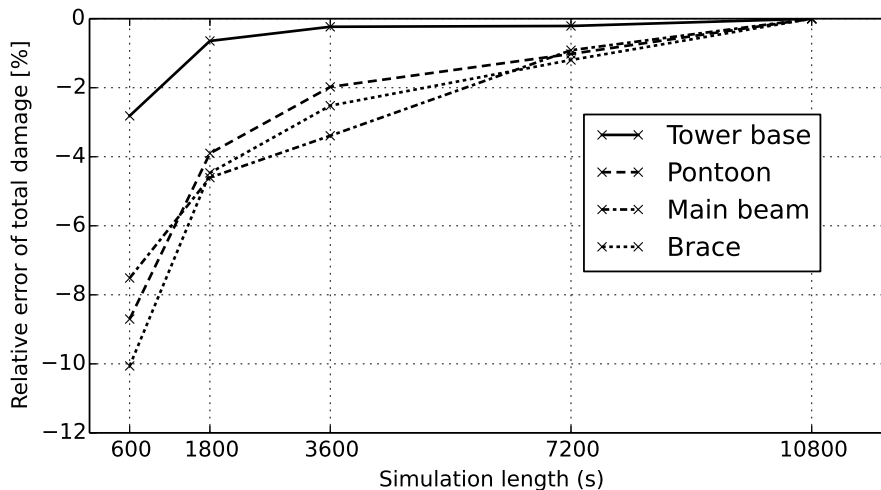


Figure 9: Relative difference to 3-hour simulations in 20 year total damage (Eq. 4) for axial stress fatigue. The average damage from 10 samples was used for all the simulation lengths shown.

In essence, a 3-hour simulation contains the same statistical content as 3x1-hour or 6x30-min simulations. I.e., using longer simulations reduces the number of seeds required. It was found that the long term fatigue damage calculated based on 10-minute simulations varied more with seed number, and gave larger errors compared to the 10 seed average than for the longer simulation lengths (Fig. 10). Another important observation is that the error for fatigue in the tower base was very small.

A full evaluation of the required number of seeds in a statistical sense would require a large sample of 3-hour simulations. A sample of 10, which was used in this study, is not statistically significant. Moreover, the fact that the order of the samples is random, contributes to the non-converging behaviour of the data in Fig. 10. The focus was kept on including as many different environmental conditions as possible within the time frame of this work, and thus the number of samples could not be increased. Therefore, a method introduced by Langley [34] to estimate the root mean square (RMS) error of a limited number of program runs (Eq. 5) was applied.

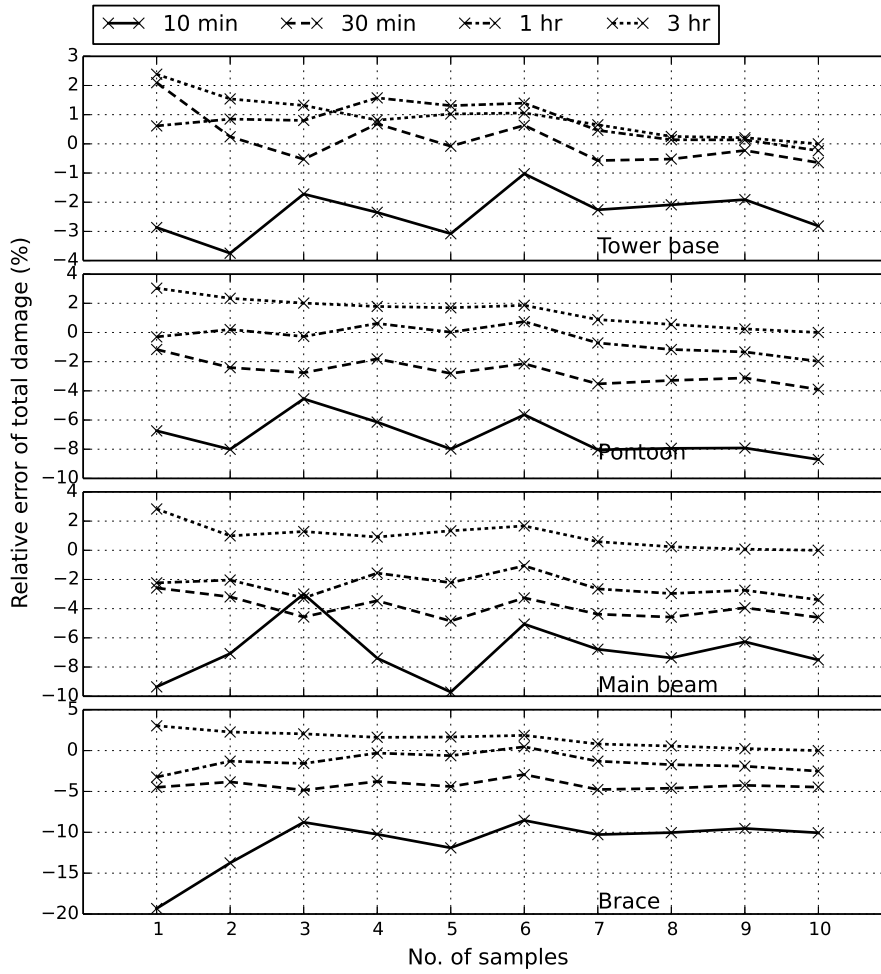


Figure 10: 20 year damage as a function of the number of samples, calculated as the cumulative average of N^{seeds} , where N^{seeds} varied from 1 to 10. The error refers to the damage calculated from 10x3-hour simulations.

$$\delta = \frac{1}{\sqrt{N^{seeds}}} \frac{\sigma_D}{\mu_D} \quad (5)$$

μ_D and σ_D in this context are the mean value and the standard deviation, respectively, of the 20 year fatigue damage.

The resulting RMS error is shown in Fig. 11. Similar conclusions to what has been described earlier in this section can be drawn from the RMS estimate; errors are small in general, but larger for 10-minute simulations, and the tower base was less sensitive to the number of seeds than the platform members.

Figure 11 also illustrates an important point; that the statistic content is the same in six 10-minute samples as in one 1-hour sample, and thus the expected error is the same.

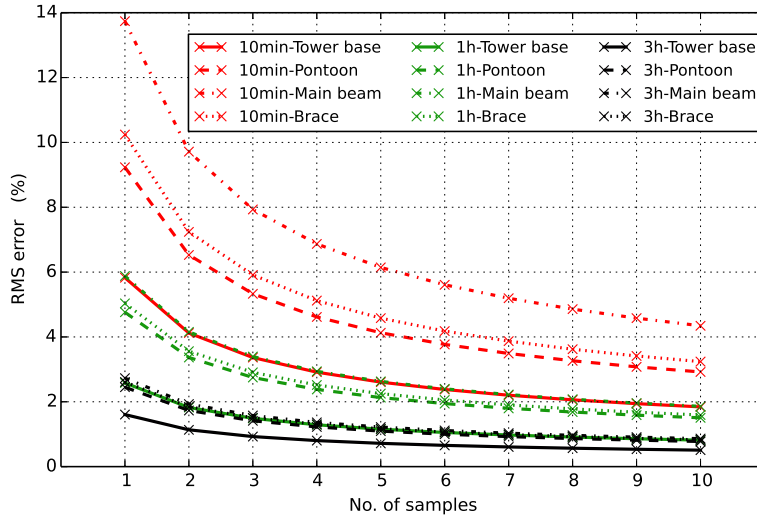


Figure 11: Estimated RMS error for 20 year damage, as a function of number of samples.

6.3 Bin size and load case selection

The discretisation of long term environmental conditions (determining bin size) must ensure that all important load effects are captured such that a realistic and conservative estimate of the fatigue damage can be determined. Moreover, a coarse grid of environmental conditions also means fewer simulations and thus fewer random samples.

In this section, the influence of bin size on the 20 year fatigue damage is investigated based on 1 realisation of the load cases labelled “additional” in Fig. 7, as well as 10 seed average damage from the load cases in Fig. 5.

6.3.1 Bin size for wind speeds

The total fatigue was calculated for increasing bin sizes. Table 6 shows that by increasing the bin size from 1 to 2 m/s, the total fatigue damage for the

tower was reduced by 9%. However, a bin size of 2 m/s, starting at cut-in wind speed (i.e. load cases include 3, 5, 7,.. m/s), means that the most important resonance case at 8 m/s is left out. If a bin size of 2 m/s was used, and the 8 m/s cases were included, the deviation in the total damages would be 0.3% for the tower, 3.2% for the pontoon, 1% for the main beam and 3.1% for the brace. This indicates that a bin size of 2 m/s will give an acceptable damage estimate if 3P resonance cases are included.

Table 6: Variation of 20 year fatigue damage in tower base for varying bin size, relative to the smallest bin size. The bin size is 1 m/s for wind speed, 0.5 m for wave height and 0.5 s for wave period, unless otherwise specified. The damage is calculated according to Eq. 6. Please note that the selection of H_s representing bin sizes below 1.5 m is limited.

Bin size U_{hub}	Tower base D_{rel} (%)	Pontoon D_{rel} (%)	Main beam D_{rel} (%)	Brace D_{rel} (%)	No. of env. cond.
1.0 m/s	100	100	100	100	478
2.0 m/s	91	90	89	88	219
3.0 m/s	88	85	79	85	152
4.0 m/s	85	83	83	81	120
<hr/>					
H_s					
0.5 m	100	100	100	100	478
1.0 m	101	101	100	99	234
1.5 m	96	94	96	94	410
2.0 m	41	38	44	38	101
<hr/>					
T_p					
0.5 s	100	100	100	100	478
1.0 s	100	100	101	100	442
1.5 s	104	103	101	103	161
2.0 s	103	105	104	104	245

The number of environmental conditions included in the calculation of the total fatigue damage for different bin sizes is shown in the rightmost column of Tab. 6. What can be observed, is that the total fatigue damage changes more from 478 to around 200 environmental conditions when changing the wind speed bin size, than when changing the wave height or wave period bin size. The relatively low sensitivity to the number of seeds, which was described in Sec. 6.2, is consistent with this. Thus, it seems that the total fatigue damage was more sensitive to the bin size parameter than the number of environmental conditions.

In the H_s section of Tab. 6, the number of environmental conditions is smaller for bin size 1.0 m than for 1.5 m. The same can be observed for T_p . This has to do with the distribution and the selection of simulated environmental conditions (as shown in Fig. 7).

6.3.2 Bin size for wave periods

To be able to evaluate if the most important wave periods are included in the total fatigue damage assessment, comparisons of damage for load cases with

varying wave period were carried out (“wave period” in Fig. 5). These comparisons indicated that pitch motion has a significant contribution to fatigue damage in all members. Figures 12 and 13 show the highest damages for 10-12 s waves, which coincides with a peak in the pitch response amplitude operator. The reduction of fatigue damage with increasing wave period in Figs. 12 and 13 is fairly linear, which can explain that the increase of wave period bin size do not cause significant changes in the damage estimates in Tab. 6. Choosing a bin size of 2 s gave an acceptable result in this case, but keep in mind that this conclusion depends on the response characteristics of the platform.

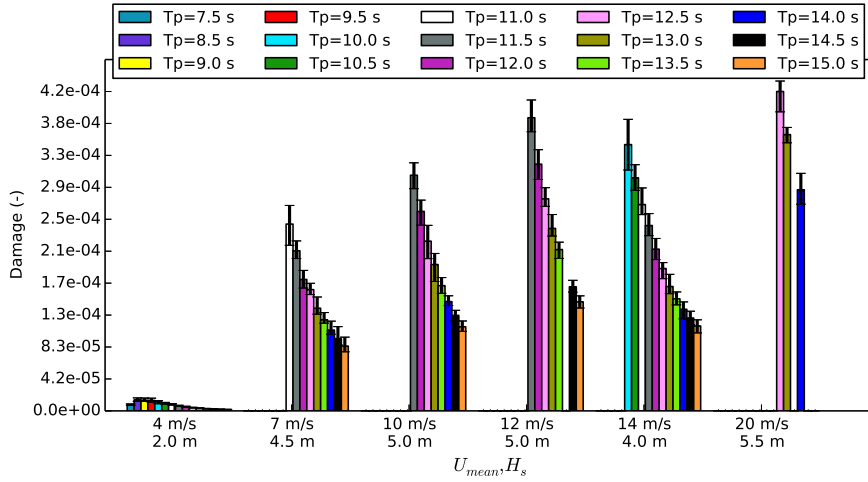


Figure 12: 3-hour short term fatigue damage due to axial stress in the tower base for varying wave period, averaged over 10 seeds. Maximum/minimum observed damage in all realisations is shown with errorbars.

The selection of load cases called “additional” in Fig. 7 has a bin size of 1 s for wave periods, which means that the damage for bin size 0.5 s in Tab. 6 does not include all possible load cases with 0.5 s bin size. However, comparing damage weighted with probability for the cases labelled “wave period” in Fig. 7 with a bin size of 1.0 s only gives 0.4-3.9% difference compared to a bin size of 0.5 s.

6.3.3 Bin size for wave heights

Table 6 indicates that 1.0 m bin size for wave heights will give acceptable results. The bin size for wave heights in the “additional” load cases (Fig. 7) is 1.5 m. Calculating fatigue for the load cases that have a bin size of 0.5 m, 1.5 m bin size gives 1.0-9.4% difference (17-32% for 4 m/s wind and 12 s waves).

One possible explanation for damage being more sensitive to the increase of bin size for wave heights can be found in the wave induced pitch motion of the platform. Assuming that only forces on the tower caused by pitch motion causes tower fatigue, and that the stresses increase linearly with pitch angle, the fatigue damage increase will be non-linear (in the order of the m-parameter in the fatigue curve, which is 3 and 5 in this study, see [28]). Nonetheless, as can be seen in Fig. 7, more cases with variation in wave height should be included

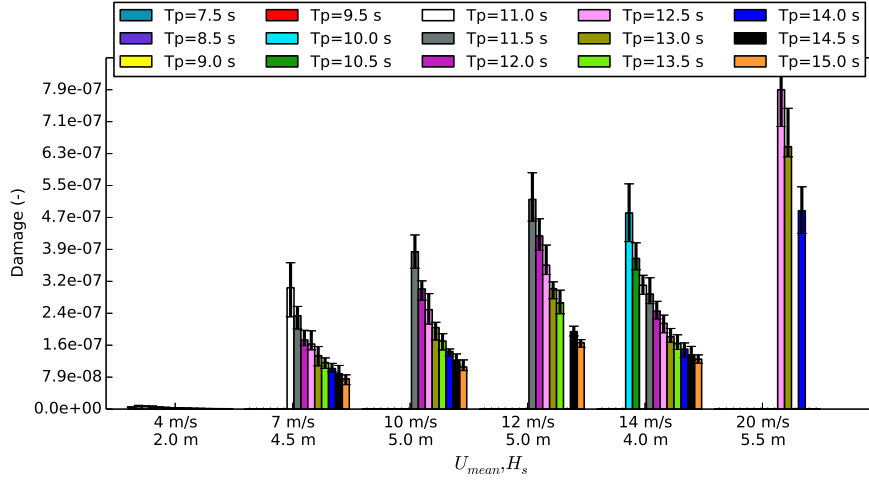


Figure 13: 3-hour short term fatigue damage due to axial stress in the brace for different wind speeds, wave heights and periods, averaged over 10 seeds. Maximum/minimum observed damage in all realisations is shown with errorbars.

to make a firm conclusion about sensitivity to wave height bin size.

6.4 Total fatigue damage for other sites

Although this study was not an attempt to do full fatigue damage assessment, and no explicit values for long term fatigue damage is presented, it should be mentioned that the calculated damages indicate an unacceptably low fatigue life, since installation, survival conditions, faults and parked condition also require parts of the allowable fatigue damage, and since weld geometries most likely will give stress concentration factors higher than 1.

In order to give an impression of how much the long term fatigue damage can be reduced by applying environmental data from other sites, sensitivity was performed by using the probability distributions from the other sites addressed in [21]. The relative total 20-year fatigue damage (Eq. 4) compared to the Portugal location was:

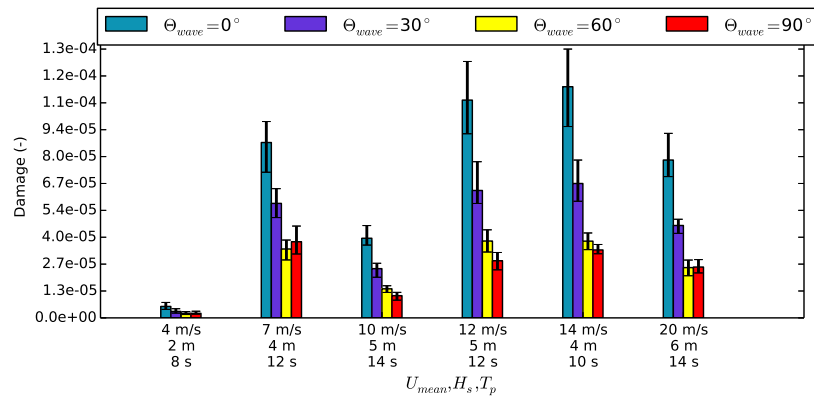
- 69-82% for site no. 1 (Atlantic, France)
- 89-94% for site no. 5 (Atlantic, Great Britain)
- 121-130% for site no. 14 (North Sea - Norway)
- 64-78% for site no. 15 (North Sea - Denmark)

The water depth in site no. 1, 5 and 15 is lower than assumed in this study, and thus they are not relevant sites for this particular SSWT, considering that the mooring design would have to be redesigned. The numbers do, however, give an idea of the sensitivity of fatigue damage to wind- and wave distribution at different sites.

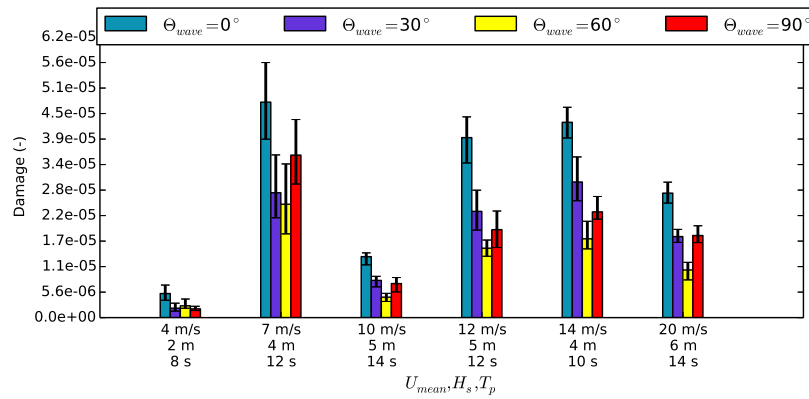
6.5 Misaligned wind and wave conditions

Uni-directional wind and waves, with long crested waves, were assumed in the above sections. Fatigue damage calculated based on misaligned wind and waves indicated that this was a conservative assumption (Fig. 14). The reason for the different conclusion in [33] and [32] will be further discussed in another paper with misalignment as the main focus [19]. In short, the bending moments from wind and waves act around different axes, and thus the contribution to fatigue damage comes in different cross section locations. This is clearly seen for the tower. Bottom fixed turbines get fatigue damage due to flexible modes, which do not have very high hydrodynamic damping. For the SSWT large contributions to fatigue damage come from the rigid body motions of the platform (roll and pitch), and these motions have high drag damping from the heave plates. Wind from other angles than 0° and 90° have not been simulated, and fatigue damage may be higher with aligned wind and waves from other angles.

Figure 14a shows an incoming wind angle of 0° , and Fig. 14b shows the 90° case, both with the rotor facing the wind (see Fig. 6 for a definition of the directions). In general, the 0° case displayed significantly higher short term damage than the 90° case, which is most likely due to the wave excitation being smaller when coming from the side. And even when the wave excitation come from the front, the wind comes from the side, and the forces act around different axes, causing less fatigue damage.



(a) Incoming wind angle 0° .



(b) Incoming wind angle 90° .

Figure 14: 1-hour fatigue damage based on axial stress in tower base for misaligned wind and waves, averaged over 10 seeds. Maximum/minimum observed damage in all realisations is shown with errorbars. A definition of directions can be seen in Fig. 6.

7 Conclusions

This study deals with fatigue analysis for a wide range of environmental conditions for a semi-submersible wind turbine with the purpose of studying the effect of simulation length, the number of necessary realisations of wind and wave loads, bin size and wind-wave misalignment.

The study showed that blade passing frequency resonance in the tower and pitch motion of the platform were the most significant contributors to fatigue damage in the tower and pontoon. Capturing resonant responses is important when choosing load cases for fatigue analysis. Choosing load cases that do not give high fatigue damage is also important, to get a realistic fatigue estimate for the service life.

Based on 10x3-hour simulations of 155 environmental conditions, the sensitivity to simulation length and number of realisations was investigated. By calculating fatigue based on 10-minute samples, fatigue damage was underestimated by up to 12%. For 1-hour durations, the estimate was 5% below the 3-hour damage. The simulations showed that the overall trend for the fatigue damage estimate decreased with number of random realisations. The RMS error compared to the average of 10 3-hour realisations was less than 1% for 7 seeds of 3-hour simulations and less than 2% for 9 seeds of 1-hour simulations. Fatigue damage in the platform members was more sensitive to the number of realisations and simulations duration than the damage in the tower base.

Based on the conclusions that only 1 3-hour realisation gave a satisfactory fatigue damage estimate, 346 additional environmental conditions were analysed to study the effect of bin size. A bin size of 2 m/s for wind speeds gave acceptable damage estimates, provided that wind speeds for the important resonance frequency at 8 m/s was included. For waves bin sizes of 1 s for T_p gave similar estimates as 0.5 s, but with respect bin size for H_s , fatigue damage was more sensitive to bin size.

Misaligned wind and waves seemed to give less fatigue than unidirectional wind and waves, which means that it is conservative to assume unidirectionality. However, which parts of the platform structure that experience the highest fatigue damage, will depend on the wave direction.

Placing a turbine on a floating platforms alters the natural frequencies of the turbine itself. For the platform in this study, the tower first fore-aft and side-to-side bending frequencies are within the range of the blade passing frequency for wind speeds 7-9 m/s. This lead to resonance in the tower for these wind speeds. At resonance it is important to have a proper representation of the aerodynamic and structural damping. This is however an issue in some state-of-the-art aerodynamic models, since BEM without dynamic wake correction does not include wake damping, and the generalised dynamic wake model in AeroDyn is unstable for wind speeds around 8 m/s and below. This calls for an improvement of aerodynamic codes applied in the analysis of floating wind turbines.

Fatigue damages observed in this study indicate that fatigue damage will be unacceptably high for the tower. Since resonant motion in the first bending frequency of the tower contributes significantly to fatigue below rated wind speed, towers should be designed for each platform type to have resonance frequencies outside of the blade passing frequency range.

8 Acknowledgements

The authors wish to acknowledge the support from NOWITECH and the Norwegian Research Council through Centre for Ships and Ocean Structures at NTNU.

References

- [1] Det Norske Veritas. *DNV-RP-J103, Design of Floating Wind Turbine Structures*, 2013.
- [2] M. Karimirad and T. Moan. Extreme dynamic structural response analysis of catenary moored spar wind turbine in harsh environmental conditions. *Journal of offshore mechanics and Arctic engineering*, 133(4), 2011.
- [3] L. Haid, G. Stewart, J. Jonkman, A. Robertson, M. Lackner, and D. Matha. Simulation-length requirements in the loads analysis of offshore floating wind turbines. In *Proceedings of the 32nd International Conference on Ocean, Offshore and Arctic Engineering*, Nantes, France, 2013.
- [4] M. I. Kvittem, T. Moan, Z. Gao, and C. Luan. Short-term fatigue analysis of semi-submersible wind turbine tower. In *Proceedings of 30th International Conference on Ocean Offshore and Arctic Engineering*, Rotterdam, The Netherlands, 2011. Paper no. OMAE2011-50278.
- [5] J. Jonkman, S. Butterfield, W. Musial, and G. Scott. Definition of a 5-MW reference wind turbine for offshore system development. Technical report, NREL, 2009. NREL/TP-500-38060.
- [6] J. Jonkman. Definition of the floating system for phase IV of OC3. Technical report, National Renewable Energy Laboratory, 2010.
- [7] D. Roddier, A. Peiffer, A. Aubault, and J. Weinstein. A generic 5MW WindFloat for numerical tool validation and comparison against a generic spar. In *Proceedings of ASME 30th International Conference on Ocean Offshore and Arctic Engineering*, Rotterdam, The Netherlands, 2011. Paper no. OMAE2011-50278.
- [8] MARINTEK. *RIFLEX User's Manual*, 2013.
- [9] MARINTEK. *SIMO User's Manual*, 2013.
- [10] D. Laino and A. C. Hansen. *AeroDyn users guide*, 2002.
- [11] H. Ormberg and E. E. Bachynski. Global analysis of floating wind turbines: Code development, model sensitivity and benchmark study. In *Proceedings of the 22nd International Ocean and Polar Engineering Conference*, Rhodes, Greece, 2012.
- [12] MARINTEK. *SIMO Theory Manual*, 2012.
- [13] Det Norske Veritas. *SESAM User Manual Wadam*, 2008.
- [14] Det Norske Veritas. *DNV-OS-E301, Offshore standard-position mooring*, 2010.
- [15] Det Norske Veritas. *DNV-RP-C205, Environmental Conditions and Environmental Loads*, 2007.
- [16] Principle Power. Wamit model for WindFloat 5 MW. Technical report, Principle Power, 2010.

- [17] C. Luan, Z. Gao, and T. Moan. Modelling and analysis of a semi-submersible wind turbine with a central tower with emphasis on the brace system. In *Proceedings of the 32nd International Conference on Ocean, Offshore and Arctic Engineering*, Nantes, France, 2013.
- [18] O. M. Faltinsen. *Sea Loads on Ships and Ocean Structures*. Cambridge University Press, 1990.
- [19] E. E. Bachynski, M. I. Kvittem, C. Luan, and T. Moan. Wind-wave misalignment effects on floating wind turbines. To be published, 2014.
- [20] A. Robertson, J. Jonkman, Musial W., F. Vorpahl, and W. Popko. Offshore code comparison collaboration, continuation: Phase II results of a floating semisubmersible wind system. Technical report, National Renewable Energy Laboratory, 2013.
- [21] L. Li, Z. Gao, and T. Moan. Joint environmental data at five european offshore sites for design of combined wind and wave energy devices. In *Proceedings of ASME 32th International Conference on Ocean Offshore and Arctic Engineering*, Nantes, France, 2013. Paper no. OMAE2013-10156.
- [22] B. J. Jonkman. *TurbSim users guide*, 2009.
- [23] International Electrotechnical Commission. *IEC61400-1, Wind turbines - Part 1: Wind turbines, design requirements*, 2005.
- [24] I. Van der Hoven. Power spectrum of horizontal wind speed in the frequency range from 0.0007 to 900 cycles per hour. *Journal of Meteorology*, 14(2):160–164, 1957.
- [25] J. Apt. The spectrum of power from wind turbines. *Journal of Power Sources*, 169(2):369–374, 2007.
- [26] T. Burton, N. Jenkins, D. Sharpe, and E. Bossanyi. *Wind energy handbook*. John Wiley & Sons, 2011.
- [27] F. Irgens. *Mechanics of Materials (in Norwegian)*. Tapir, 2006.
- [28] Det Norske Veritas. *DNV-RP-C203, Fatigue Design of Offshore Steel Structures*, 2010.
- [29] Det Norske Veritas. *DNV-RP-J101, Design of Offshore Wind Turbine Structures*, 2010.
- [30] International Electrotechnical Commission. *IEC61400-3, Wind turbines - Part 3: Design requirements for offshore wind turbines*, 2009.
- [31] Det Norske Veritas. *DNV-RP-C103, Column-stabilised units*, 2010.
- [32] T. Fischer, W. Vries, P. Rainey, B. Schmidt, K. Argyriadis, and M. Kühn. Offshore support structure optimization by means of integrated design and controls. *Wind Energy*, 15(1):99–117, 2012.

- [33] L. Barj, S. Stewart, G. Stewart, M. Lackner, J. Jonkman, A. Robertson, L. Haid, and D. Matha. Impact of wind/wave misalignment in the loads analysis of a floating wind turbine. In *Poster presentation at AWEA Wind Power*, 2013.
- [34] R. S. Langley. On the time domain simulation of second order wave forces and induced responses. *Applied ocean research*, 8(3):134–143, 1986.